



Glacier Extent During the Younger Dryas and 8.2-ka Event on Baffin Island, Arctic Canada

Nicolás E. Young *et al.*
Science **337**, 1330 (2012);
DOI: 10.1126/science.1222759

This copy is for your personal, non-commercial use only.

If you wish to distribute this article to others, you can order high-quality copies for your colleagues, clients, or customers by [clicking here](#).

Permission to republish or repurpose articles or portions of articles can be obtained by following the guidelines [here](#).

The following resources related to this article are available online at www.sciencemag.org (this information is current as of September 17, 2012):

Updated information and services, including high-resolution figures, can be found in the online version of this article at:

<http://www.sciencemag.org/content/337/6100/1330.full.html>

Supporting Online Material can be found at:

<http://www.sciencemag.org/content/suppl/2012/09/12/337.6100.1330.DC1.html>

This article **cites 51 articles**, 6 of which can be accessed free:

<http://www.sciencemag.org/content/337/6100/1330.full.html#ref-list-1>

This article appears in the following **subject collections**:

Atmospheric Science

<http://www.sciencemag.org/cgi/collection/atmos>

Glacier Extent During the Younger Dryas and 8.2-ka Event on Baffin Island, Arctic Canada

Nicolás E. Young,^{1*†} Jason P. Briner,¹ Dylan H. Rood,^{2,3} Robert C. Finkel⁴

Greenland ice cores reveal that mean annual temperatures during the Younger Dryas (YD) cold interval—about 12.9 to 11.7 thousand years ago (ka)—and the ~150-year-long cold reversal that occurred 8.2 thousand years ago were ~15° and 3° to 4°C colder than today, respectively. Reconstructing ice-sheet response to these climate perturbations can help evaluate ice-sheet sensitivity to climate change. Here, we report the widespread advance of Laurentide Ice Sheet outlet glaciers and independent mountain glaciers on Baffin Island, Arctic Canada, in response to the 8.2-ka event and show that mountain glaciers during the 8.2-ka event were larger than their YD predecessors. In contrast to the wintertime bias of YD cooling, we suggest that cooling during the 8.2-ka event was more evenly distributed across the seasons.

Summit Greenland ice cores record several abrupt cold excursions that occurred throughout the last glacial period and into the early Holocene (1, 2). Characterized by rapid onset and termination times, the Younger Dryas (YD) and the excursion that occurred 8.2 thousand years ago (ka) are two of the most dramatic examples of abrupt climate change, and consequently their intra- and interhemispheric signature has been the subject of intense focus [e.g., (3, 4)]. Characterizing the extent and magnitude of abrupt climate events beyond their central Greenland stratotypes is critical for understanding the mechanisms that drive abrupt climate change and for understanding how regional climate-system changes are transmitted globally via atmospheric and oceanic teleconnections.

The expression of the YD outside central Greenland has proven particularly puzzling. Even on Greenland, independent terrestrial proxy records that track changes in summer climate do not replicate the extreme temperature depression of the YD depicted in Greenland ice [e.g., (5)]. This disparity has led to the hypothesis that the YD and other abrupt cold reversals in the North Atlantic region were typified by strong seasonality, with cooling primarily restricted to the wintertime and only minimal to moderate summer cooling (6, 7). To test this hypothesis, proxies for terrestrial climate change need to be generated from elsewhere in the North Atlantic region.

Located directly adjacent to Greenland, Baffin Island hosts remnants of the Laurentide Ice Sheet

(LIS) and numerous mountain glaciers whose late glacial to early Holocene histories have remained relatively unexploited compared with their counterparts in Europe [e.g., (8)]. An extensive moraine system deposited along eastern Baffin Island fjord heads was originally believed to demarcate the late Wisconsin maximum extent of the LIS (Fig. 1) (9, 10). Recent work, however, has demonstrated that during the late Wisconsin, the LIS extended to at least the fjord mouths and likely out onto the Baffin Bay continental shelf, with regional deglaciation commencing ~15 to 16 ka (11, 12). Thus, fjord-head moraines represent an advance of the LIS superimposed on deglaciation. Considered correlative with this ice limit are moraines that were deposited by local mountain glaciers that became independent of the LIS during deglaciation (10). Fjord-head moraines are currently dated with conventional

radiocarbon ages from marine fauna that broadly constrain moraine deposition to ~8 to 9.5 thousand calibrated years before the present (cal yr B.P.) (Cockburn Substage) (13); this chronology has remained relatively unchanged for three decades. Here, we precisely date mountain-glacier moraines deposited during the Cockburn Substage on Baffin Island using ¹⁰Be surface exposure dating and compare our new chronology to ¹⁰Be- and ¹⁴C-dated fluctuations of nearby LIS outlet glaciers (Fig. 1).

Our chronology arises from mountain-glacier moraines deposited in Ayr Lake valley after Laurentide ice, which occupied the valley during the last glaciation, retreated during deglaciation. ¹⁰Be ages from the Clyde Foreland and Ayr Lake valley, calculated with a locally constrained ¹⁰Be production rate (14), indicate that the LIS retreated from the Clyde Foreland 14.1 ± 1.2 ka ($n = 7$ ¹⁰Be ages; mean ± 1 SD), through Ayr Lake valley at 13.7 ± 0.1 ka ($n = 3$ ¹⁰Be ages), and well inland of the study area by 12.7 ± 0.3 ka ($n = 1$ ¹⁰Be ages) (Fig. 2) (14). Thus, tributary glaciers extending from adjacent ice caps flanking Ayr Lake valley disconnected from the LIS outlet glacier ~13.7 ± 0.1 ka. We dated boulders from two correlative moraines deposited in Ayr Lake valley by mountain glaciers during the Cockburn Substage (Fig. 2). Both moraines, ~20 km apart, have mature lichen cover and are situated immediately down-valley of unvegetated, fresh-appearing moraines that we assume were deposited during the late Holocene. ¹⁰Be ages from moraine boulders range from 17.2 ± 0.3 to 7.9 ± 0.2 ka ($n = 13$ ¹⁰Be ages). Two boulder ages of 17.2 ± 0.3 and 14.2 ± 0.3 ka are >3 SD older than the remaining ¹⁰Be ages and likely contain ¹⁰Be inherited from previous exposure, which is widespread in this region outside of valley bottoms (12, 14). The remaining 11 ¹⁰Be ages indicate that an advance

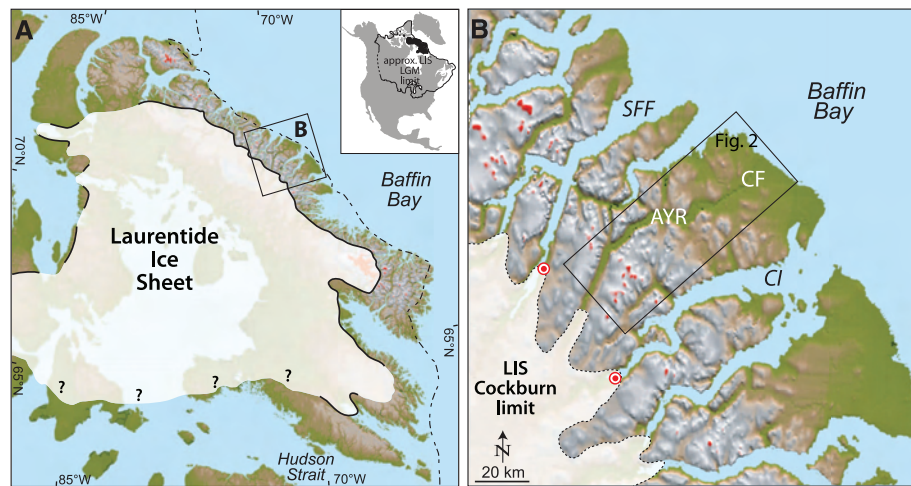


Fig. 1. (A) Late Wisconsin extent of the LIS [dashed line; modified from (12, 35)] and the extent of the fjord-head Cockburn moraine system (9, 10, 13). Green and red on basemaps are lowest and highest elevations, respectively. (B) LIS Cockburn limit in central Baffin Island. AYR, Ayr Lake valley; CI, Clyde Inlet; SFF, Sam Ford Fiord; CF, Clyde Foreland. Red bull's eyes mark the position of 8.2-ka ice-contact deltas in Sam Ford fiord and Clyde Inlet (Fig. 3).

¹Department of Geology, University at Buffalo, 411 Cooke Hall, Buffalo, NY 14260, USA. ²Accelerator Mass Spectrometry Laboratory, Scottish Universities Environmental Research Centre (SUERC), East Kilbride, UK. ³Earth Research Institute, University of California, Santa Barbara, CA 93106, USA. ⁴Department of Earth and Planetary Sciences, University of California—Berkeley, Berkeley, CA 94720, USA.

*To whom correspondence should be addressed. E-mail: nicolas@ldeo.columbia.edu

†Present address: Lamont-Doherty Earth Observatory, Columbia University, New York, NY 10964, USA.

of mountain glaciers in Ayr Lake valley culminated $\sim 8.2 \pm 0.2$ ka (Figs. 2 and 3).

Additional ^{10}Be and ^{14}C ages from the heads of Clyde Inlet and Sam Ford fjord constrain early Holocene fluctuations of the LIS (Figs. 1B and 3). In Clyde Inlet, ^{10}Be ages from boulders atop an ice-contact delta range from 8.6 ± 0.6 to 7.5 ± 0.8 ka and have a mean age of 8.0 ± 0.4 ka ($n = 7$ ^{10}Be ages) (Fig. 3) (15). This age assignment agrees with independent ^{14}C ages that bracket deposition of the ice-contact delta to between 8435 ± 30 and 7950 ± 45 cal yr B.P. (1 SD) (14). In Sam Ford fjord, numerous ^{10}Be ages indicate that the majority of the fjord rapidly deglaciated 9.5 ± 0.3 ka but did not deglaciate completely until after ~ 7.7 ka (16). Radiocarbon ages of 8330 ± 30 and 8210 ± 190 cal yr B.P. from an ice-contact delta deposited during the Cockburn Substage mark the timing of a readvance by the LIS outlet glacier occupying Sam Ford fjord (14).

Taken together, ^{10}Be and ^{14}C ages from Ayr Lake valley, Clyde Inlet, and Sam Ford fjord indicate that a synchronous advance of mountain glaciers and LIS outlets occurred between ~ 8.3 and 8.0 ka, probably driven by the 8.2-ka abrupt cold reversal displayed in Greenland ice cores (Fig. 3). In some locations, several distinct ice limits associated with the Cockburn Substage are identifiable (e.g., Sam Ford fjord) (17), indicating that the 8.2-ka event glacier response may be superimposed upon a broader pattern of glacier advance

and retreat between ~ 9.5 and 8 thousand cal yr B.P. whose climatic importance, if any, remains unclear. Nonetheless, the 8.2-ka event cooling was sufficient to trigger a widespread response of eastern Baffin Island glaciers, perhaps correlative with early Holocene advances of the western Greenland Ice Sheet (18). In addition, the 8.2-ka event triggered an advance of the eastern LIS indicating that ice sheets are capable of an extremely rapid glaciological response (i.e., centennial-scale or less) to a short-lived climate perturbation.

Because the 8.2-ka moraines rest directly on the Ayr Lake valley floor that deglaciated ~ 14 to 13 ka, 8.2-ka event moraines mark the most extensive limit of local mountain glaciers since ~ 14 ka. Therefore, our chronology indicates that mountain glaciers were larger during the 8.2-ka event than during the YD. Although our chronology does not preclude a YD-triggered advance of Ayr Lake mountain glaciers, the morphostratigraphic relationship between the 8.2-ka moraines and the Ayr Lake valley floor requires glaciers during the YD to have been less extensive than they were during the 8.2-ka event. The larger response of Baffin Island glaciers to the 8.2-ka event relative to the YD is surprising considering the significantly longer duration and greater amplitude of YD temperature change compared with the 8.2-ka event.

The absence of a distinct YD moraine on Baffin Island is not necessarily unexpected. For

example, unequivocal YD moraines in the Northern Hemisphere have not been identified outside northern Europe, and in the Southern Hemisphere mid-latitudes, glaciers appear to have advanced before, and then retreated during, the YD interval (4, 19). On eastern Greenland, a major moraine complex brackets the YD but, perhaps more importantly, indicates that YD summertime cooling was only 3.9° to 6.6°C relative to today (7), much less than the $\sim 15^\circ\text{C}$ mean annual cooling recorded in central Greenland ice cores by gas-fractionation paleothermometry (2).

An independent proxy record from Lake CF8 in our study area indicates that summer temperatures during the 8.2-ka event lowered by $\sim 3.5^\circ\text{C}$ (20) (Figs. 2 and 3). At high northern latitudes, $\sim 90\%$ of the variability in glacier mass balance is controlled by ablation-season (summer) temperature (21), and thus summertime cooling of $\sim 3.5^\circ\text{C}$ during the 8.2-ka event helped drive eastern Baffin Island mountain glaciers to advance beyond their YD limit. Precipitation rates during the YD, however, were up to ~ 50 to 100% less than early Holocene values (22, 23) and likely contributed to a restricted YD ice extent. Because a ~ 40 to 50% change in precipitation is equivalent to a $\sim 1^\circ\text{C}$ temperature change (24, 25), we constrain the magnitude of summer cooling during the YD on eastern Baffin Island to have been no more than $\sim 4.5^\circ$ to 5.5°C . This level of summer cooling during the YD is consistent

Fig. 2. (A) The Clyde Foreland with recessional ice limits (11) and Ayr Lake valley with ^{10}Be ages (ka) (1 SD analytical uncertainty) that constrain retreat of the LIS outlet glacier through Ayr Lake valley. (B and C) ^{10}Be ages from moraine boulders deposited by local mountain glaciers.



with strong seasonality when considering the $\sim 15^{\circ}\text{C}$ mean annual cooling recorded in Greenland ice cores (6).

In contrast, the 3.5°C of summer cooling recorded on Baffin Island during the 8.2-ka event is indistinguishable from central Greenland mean annual temperatures depicting a peak 8.2-ka temperature depression of $\sim 3^{\circ}$ to 4°C (26, 27) (Fig. 3). Furthermore, terrestrial proxy records and model simulations of the 8.2-ka event climate [e.g., (3)] typically assert that maximum cooling in the North Atlantic region occurred downstream (east) of the 8.2-ka event's epicenter in the Labrador Sea due to westerly atmospheric and oceanic circulation patterns. Deposition of the Cockburn moraines on Baffin Island, combined with the independent summer temperature reconstruction from the Clyde Foreland, indicates that significant summer cooling during the 8.2-ka event extended west of the Labrador Sea. Unlike YD cooling, cooling during the 8.2-ka event included a significant summer component, and we suggest that the difference in mountain-glacier response between the YD and the 8.2-ka event was due to contrasting seasonality. What remains unclear, however, is the driving mechanism(s) that would allow for the 8.2-ka event to have a proportionally stronger summer-based regional cooling signature than the YD, because both cold reversals are thought to have shared similar reorganizations of North Atlantic thermohaline circulation and concomitant expansion in sea-ice coverage (3, 6, 28).

One explanation may involve each cold period's triggering mechanism. The 8.2-ka event is linked to the catastrophic drainage of Laurentide-dammed lakes and routing of meltwater through the Hudson Strait directly into the Labrador Sea (29). Accordingly, the sharp isotopic onset of the 8.2-ka event in Greenland ice cores is consistent with rapid North Atlantic freshening. The origin of the YD, however, remains debated [e.g., (28)]. Although one of several possible YD triggers invokes the sudden release of North American meltwater into the North Atlantic, no geomorphic evidence lending support to this hypothesis has been identified (30), and compared to the 8.2-ka event's onset, the beginning of the YD is less notably abrupt and succeeds a millennial-scale cooling trend (28). It has also been suggested that a Heinrich ice armada outburst (i.e., Heinrich event H0) occurred in Baffin Bay at the onset of the YD (31). However, because multiple Heinrich events occurred through the last glacial period, a Heinrich-related YD triggering mechanism would indicate that the YD is not the product of a one-time catastrophic event (28) but rather the result of a reoccurring pacemaker. Moreover, stalagmite $\delta^{18}\text{O}$ records suggest that the YD and previous YD-like events are inherent, nonstochastic components of ice-age terminations (32).

Each cold reversal's unique isotopic expression suggests differing causations and possibly different hemispheric climatic imprints. The sud-

den influx of freshwater into the Labrador Sea resulted in significant summer cooling in the Baffin Bay region during the 8.2-ka event, whereas an alternative YD triggering mechanism may have led to comparatively restricted YD summer cooling in Baffin Bay. Indeed, a recent climate model simulation of the 8.2-ka event depicts a strengthened North Atlantic subpolar gyre with maximum sea-surface cooling occurring along the western edge of the gyre (33). Furthermore, an open Nares Strait channeling frigid Arctic waters into the region, and multiple pre-8.2-ka freshwater outbursts into the Labrador Sea, likely resulted in a preconditioned Baffin Bay climate system that crossed a threshold during the 8.2-ka event, resulting in strong regional cooling (34).

Our results provide direct age limits for the Cockburn moraine system deposited by the LIS

and local mountain glaciers and highlight the importance of generating regional records of climate variability spanning intervals of abrupt climate change. The severity of the YD compared with the 8.2-ka event is obvious in central Greenland, yet our results indicate that the latter resulted in more extended Baffin Island mountain glaciers, perhaps due to different triggering mechanisms and unique pre-8.2-ka event climatic baseline conditions in the Baffin Bay region. In addition, the comparatively restricted YD summer cooling on Baffin Island reinforces the broader pattern of mild YD summers in Greenland-proximal locations (5, 7). The amplitude of Baffin Island summer temperature depression during the 8.2-ka event is similar to the drop in Greenland mean annual temperature, indicating a fundamental contrast in seasonality between YD and 8.2-ka event climates.

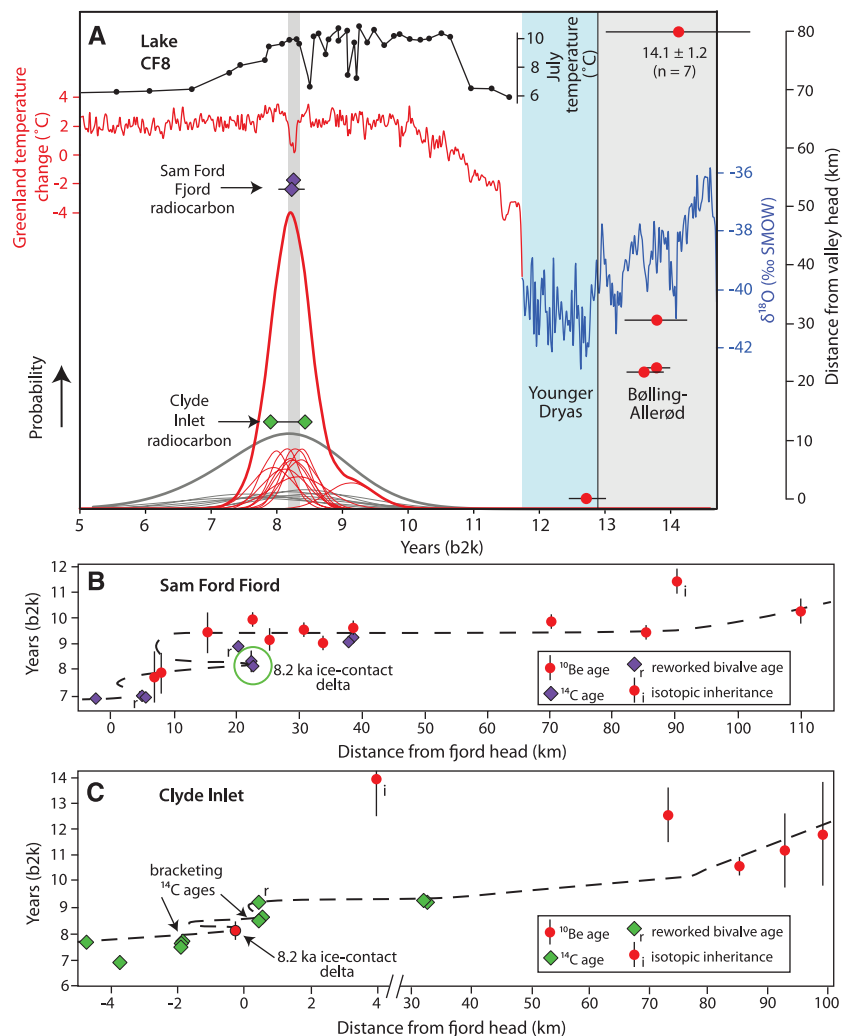


Fig. 3. (A) Ayr Lake valley ^{10}Be ages plotted as distance from the valley head. The normal kernel density estimate depicts individual and summed ^{10}Be ages from Ayr Lake moraine boulders (red) and boulders atop the Clyde Inlet ice-contact delta (gray). Results from central Baffin Island are compared to Greenland isotopic (North Greenland Ice Core Project) and elevation-corrected temperature records (27, 36) and to a local summer temperature reconstruction (Lake CF8) (19). **(B and C)** The full deglaciation histories of Sam Ford fjord and Clyde Inlet (14–16). ^{14}C ages that directly relate to 8.2-ka ice-contact deltas are highlighted and also presented in (A) (14).

References and Notes

- R. B. Alley *et al.*, *Geology* **25**, 483 (1997).
- J. Severinghaus, T. Sowers, E. J. Brook, R. B. P. Alley, M. L. Bender, *Nature* **391**, 141 (1998).
- R. B. Alley, A. M. Águústadóttir, *Quat. Sci. Rev.* **24**, 1123 (2005).
- M. R. Kaplan *et al.*, *Nature* **467**, 194 (2010).
- S. Björck *et al.*, *Geology* **30**, 427 (2002).
- G. H. Denton, R. B. Alley, G. C. Comer, W. S. Broecker, *Quat. Sci. Rev.* **24**, 1159 (2005).
- M. A. Kelly *et al.*, *Quat. Sci. Rev.* **27**, 2273 (2008).
- O. S. Lohne, J. Mangerud, J. I. Svendsen, *J. Quat. Sci.* **27**, 81 (2012).
- G. Falconer, J. T. Andrews, J. D. Ives, *Science* **147**, 608 (1965).
- G. H. Miller, A. S. Dyke, *Geology* **2**, 125 (1974).
- J. P. Briner, G. H. Miller, P. T. Davis, R. C. Finkel, *Can. J. Earth Sci.* **42**, 67 (2005).
- J. P. Briner, G. H. Miller, P. Thompson Davis, R. C. Finkel, *Geol. Soc. Am. Bull.* **118**, 406 (2006).
- J. T. Andrews, J. D. Ives, *Arct. Alp. Res.* **10**, 617 (1978).
- Materials and methods are available as supplementary materials on Science Online
- J. P. Briner, I. Overeem, G. Miller, R. Finkel, *J. Quat. Sci.* **22**, 223 (2007).
- J. P. Briner, A. C. Bini, R. S. Anderson, *Nat. Geosci.* **2**, 496 (2009).
- J. E. Smith, Sam Ford Fiord: A study in deglaciation. Thesis, McGill University, Montreal (1966).
- N. E. Young *et al.*, *Geophys. Res. Lett.* **38**, L24701 (2011).
- A. E. Putnam *et al.*, *Nat. Geosci.* **3**, 700 (2010).
- Y. Axford, J. P. Briner, G. H. Miller, D. Francis, *Quat. Res.* **71**, 142 (2009).
- R. M. Koerner, *Ann. Glaciol.* **42**, 417 (2005).
- W. R. Kapsner, R. B. Alley, C. A. Shuman, S. Anandakrishnan, P. M. Grootes, *Nature* **373**, 52 (1995).
- R. B. Alley, *Quat. Sci. Rev.* **19**, 213 (2000).
- J. Oerlemans, *Glaciers and Climate Change* (A. A. Balkema Publishers, Lisse, 2001).
- R. B. Alley, *Eos Trans.* **84**, 315 (2003).
- T. Kobashi, J. P. Severinghaus, E. J. Brook, J. M. Barnola, A. M. Grachev, *Quat. Sci. Rev.* **26**, 1212 (2007).
- B. M. Vinther *et al.*, *Nature* **461**, 385 (2009).
- W. S. Broecker *et al.*, *Quat. Sci. Rev.* **29**, 1078 (2010).
- D. C. Barber *et al.*, *Nature* **400**, 344 (1999).
- T. V. Lowell *et al.*, *Eos. Trans.* **86**, 365 (2005).
- J. T. Andrews *et al.*, *Paleoceanography* **10**, 943 (1995).
- H. Cheng *et al.*, *Science* **326**, 248 (2009).
- A. Born, A. Levermann, *Geochem. Geophys. Geosyst.* **11**, Q06011 (2010).
- C. Hillaire-Marcel, A. de Vernal, D. J. W. Piper, *Geophys. Res. Lett.* **34**, L15601 (2007).
- A. S. Dyke *et al.*, *Quat. Sci. Rev.* **21**, 9 (2002).
- S. O. Rasmussen *et al.*, *J. Geophys. Res.* **111**, (D6), D06102 (2006).

Acknowledgments: We thank M. Badding, D. Bedard, S. McGrane, N. Michelutti, and E. Thomas, who aided in sample collection. We also thank G. Miller for insightful discussions and the helpful comments from two anonymous reviewers. This work was funded in part by U.S. National Science Foundation awards ARC-909334, BCS-1002597, and BCS-752848 to J.P.B.

Supplementary Materials

www.sciencemag.org/cgi/content/full/337/6100/1330/DC1

Materials and Methods

Figs. S1 to S4

Tables S1 to S3

References (37–55)

2 April 2012; accepted 21 August 2012
10.1126/science.1222759

Initiation of Cell Wall Pattern by a Rho- and Microtubule-Driven Symmetry Breaking

Yoshihisa Oda^{1,2*} and Hiroo Fukuda^{1*}

A specifically patterned cell wall is a determinant of plant cell shape. Yet, the precise mechanisms that underlie initiation of cell wall patterning remain elusive. By using a reconstitution assay, we revealed that ROPGEF4 (Rho of plant guanine nucleotide exchange factor 4) and ROPGAP3 [ROP guanosine triphosphatase (GTPase)-activating protein 3] mediate local activation of the plant Rho GTPase ROP11 to initiate distinct pattern of secondary cell walls in xylem cells. The activated ROP11 recruits MIDD1 to induce local disassembly of cortical microtubules. Conversely, cortical microtubules eliminate active ROP11 from the plasma membrane through MIDD1. Such a mutual inhibitory interaction between active ROP domains and cortical microtubules establishes the distinct pattern of secondary cell walls. This Rho-based regulatory mechanism shows how plant cells initiate and control cell wall patterns to form various cell shapes.

Cell shape is the basis of behavior and function of specialized cells in multicellular organisms. The plasma membrane plays central roles in the development of the functional and structural polarization of the cell. In plants, plasma membrane polarization leads to the formation of the locally specialized architecture of cell walls, resulting in various shapes of plant cells with specific functions (1–4). However, how local domains in the plasma membrane are formed and how they control local cell wall architecture in conjunction with the cytoskeleton remain a mystery. The plant-specific microtubule

binding protein MIDD1 is anchored to the plasma membrane domains and promotes local microtubule disassembly, forming a specific pattern of secondary walls in xylem vessel cells (5). MIDD1 binds Rho guanosine triphosphatases (GTPases) (6–8), which regulate cell polarization in diverse organisms (1, 9, 10). We found four ROP (Rho of plants) GTPases that were expressed in xylem cells on the basis of a metaxylem vessel-related gene expression database (11). Because of difficulty in direct observation of subcellular localization of these ROPs in developing xylem cells in situ, we observed green fluorescent protein (GFP)-ROPs expressed under the control of an estrogen-inducible system (12) in *in vitro Arabidopsis* metaxylem cell culture (5). Only GFP-ROP11 showed colocalization with filamentous structures in secondary wall pits (fig. S1, A to C). Time-lapse observation revealed that GFP-ROP11 accumulated at the end of filaments (fig. S1D), as does MIDD1 (5). Double label-

ing confirmed the colocalization of GFP-ROP11 and tag red fluorescent protein (tagRFP)-MIDD1 (Fig. 1A). In nonxylem cells, which normally lack MIDD1, GFP-ROP11 was localized along a filamentous structure only when MIDD1 was ectopically coexpressed (fig. S2A). Thus, MIDD1 can recruit ROP11 along cortical microtubules. The N-terminal domain of MIDD1 binds to microtubules, and the C-terminal domain of MIDD1 is anchored to the plasma membrane in the secondary wall pits (5). To determine whether ROP11 can recruit MIDD1 to the plasma membrane, we introduced tagRFP-MIDD1^{AN} together with GFP-ROP11, a fusion protein of GFP and a constitutive active form of ROP11 (GFP-ROP11^{G17V}), or a fusion protein of GFP and a constitutive negative form of ROP11 (GFP-ROP11^{T22N}) (13) into nonxylem cultured cells, which normally lack MIDD1. tagRFP-MIDD1^{AN} colocalized with GFP-ROP11^{G17V} and GFP-ROP11 on the plasma membrane but not with GFP-ROP11^{T22N} (fig. S2B). Thus, the GTP-bound form of ROP11 can recruit MIDD1 to the plasma membrane. Introduction of a constitutive active ROP11 (GFP-ROP11^{G17V} or GFP-ROP11^{Q66L}), but not GFP-ROP11, into differentiating metaxylem cells disrupted the pit-specific localization of MIDD1^{AN} such that distribution of MIDD1^{AN} became uniform (fig. S3) and secondary walls were formed throughout the cell surface (Fig. 1, B and C). Transgenic *Arabidopsis* plants expressing *LexA* (operator of bacterial repressor)::GFP-ROP11^{G17V} or *LexA*::GFP-ROP11^{Q66L} also exhibited disorganized secondary walls without obvious pits in metaxylem vessels, although the secondary wall pattern of protoxylem vessels was not visibly affected (fig. S4). A bimolecular fluorescence complementation (BiFC) assay using ROP11 fused with the C-terminal half of yellow fluorescent protein (cYFP-ROP11) and MIDD1^{AN} fused with the N-terminal half of YFP (nYFP-MIDD1^{AN}) in leaf epidermis revealed that nYFP-MIDD1^{AN}

¹Department of Biological Sciences, Graduate School of Science, The University of Tokyo, 7-3-1, Hongo, Bunkyo-ku, Tokyo 113-0033, Japan. ²Japan Science and Technology Corporation (JST), PRESTO, 4-1-8, Honcho, Kawaguchi, Saitama 332-0012, Japan.

*To whom correspondence should be addressed. E-mail: oda@biol.s.u-tokyo.ac.jp (Y.O.); fukuda@biol.s.u-tokyo.ac.jp (H.F.)



Supplementary Materials for

Glacier Extent During the Younger Dryas and 8.2-ka Event on Baffin Island, Arctic Canada

Nicolás E. Young,* Jason P. Briner, Dylan H. Rood, Robert C. Finkel

*To whom correspondence should be addressed. E-mail: nicolasy@ldeo.columbia.edu

Published 14 September 2012, *Science* **337**, 1330 (2012)

DOI: 10.1126/science.1222759

This PDF file includes:

Materials and Methods

Figs. S1 to S4

Tables S1 to S3

References

Materials and methods

Geologic and geomorphic setting

Bedrock in the study area primarily consists of Archean monzogranite, granodiorite, tonalite gneiss, and Proterozoic banded migmatite (12, 37). During the Last Glacial Maximum, Ayr Lake valley, Sam Ford Fiord and Clyde Inlet served as major conduits for Laurentide Ice Sheet outlet glaciers draining the ice-sheet interior. Local topographic relief from fiord/valley bottoms to adjacent valley walls generally range from ~500 - >1000 m asl and areas resting above ~1000 m asl are presently glaciated. Along the outer reaches of valleys and fiords, the landscape transitions into a relatively flat coastal lowland with elevations ranging from <100 – 200 m asl.

The terrain in the field area is typical of the eastern Canadian Arctic, categorized by a landscape of selective linear erosion (38). The uplands host block fields, tors and surfaces with weathering pits and raised quartz veins. In contrast, bedrock at lower elevations, such as valley floors, fiord-bottom islands, and raised bedrock “shoulders” resting slightly above valley and fiord bottoms, have been recently ice-sculpted and commonly display striations. To constrain the timing of Ayr Lake valley deglaciation, we focused on samples from low elevations, which are not likely to contain ^{10}Be inheritance based on our extensive work in this area (Fig. S1; 11, 12, 15, 16, 39-41). One example is a ^{10}Be -based deglaciation chronology from Sam Ford fiord where low-elevation bedrock samples were, in almost all cases, found to have no isotopic inheritance (16).

Moraine mapping presented in Figure 2 of the main text was conducted on aerial photographs and checked in the field. All moraines were visited in the field during April and May of 2008 and 2009.

Sample collection and ^{10}Be age assumptions

The location of each sample was recorded with a handheld GPS receiver with a vertical uncertainty of ~ 10 m, corresponding to a $<1\%$ uncertainty in ^{10}Be age. Boulder dimensions were measured and all samples were collected from the uppermost boulder surface using a hammer and chisel; we avoided sampling from boulder edges. The thickness of each sample was recorded and a clinometer was used to measure sample-specific shielding by the surrounding topography (Table S1). All sampled boulders were resting directly on moraine crests and boulder heights ranged from ~ 1.25 - 3.0 m above the moraine crest surface (Fig. S2; Fig. S3; Fig S4).

Crystalline bedrock and boulder lithologies in Ayr Lake valley are resistant to erosion and sampled bedrock and boulder surfaces commonly displayed glacial striations suggesting little, if any, surface erosion has occurred since deglaciation. Thus, we consider the effects of erosion on calculated ^{10}Be ages to be negligible, particularly over the relatively short (Holocene) timescales discussed here. No correction for snow cover was applied. All of our samples come from windswept locations and all sample surfaces were snow-free at the time of collection, which occurred during the time of maximum snow cover on Baffin Island (spring season).

Because our study area has undergone post-glacial isostatic uplift since deglaciation, the present sample elevation does not necessarily reflect their time-averaged sample elevation history. Unfortunately, the exact post-glacial isostatic uplift history of Ayr Lake valley is not known. The marine limit on the coastal lowland, ~ 25 km beyond Ayr lake and farther from the ice-sheet source, is 22 m asl and dates to ~ 16 ka (11, 41); the marine limit at the head of Clyde Inlet, ~ 40 km to the southwest, and closer to the ice-sheet source than our Ayr Lake sample locations, is 67 m asl and dates to ~ 8500 cal yr BP (15). These emergence data, combined with

the pattern of uplift isobases (10), indicate that our samples >10 ka underwent no more than ~22 m of uplift (marine limit at the Clyde Foreland; 11), and the Holocene moraine boulder samples experienced no more than ~40-60 m of uplift. Thus the elevation correction for Clyde Foreland and Ayr Lake deglaciation samples amounts to <1% increase in ^{10}Be age (18), and for moraine boulders deposited ~8 ka, the elevation correction results in a ^{10}Be age that is <1% older than ^{10}Be ages calculated without an elevation correction. For samples located on the Clyde Foreland the correction for ^{10}Be ages range from 0.09-0.11% and average 0.10%. For moraine boulders, ^{10}Be age corrections range from 0.53-0.58% and average 0.56%. For comparison, samples from Norway that had an ~11.6 ka exposure history, had undergone ~70 m of rebound and were from low elevations similar to our Ayr Lake valley samples, required a correction in ^{10}Be concentrations of only ~1-2% (42). Boulders deposited in Ayr Lake valley experiencing ~8 ka of exposure and having only undergone 40-60 m of uplift would likely require a smaller ^{10}Be age correction, supported by our estimated ^{10}Be age correction (<1%). Nonetheless, our elevation corrections fall within our vertical GPS uncertainty and therefore we did not apply a sample elevation correction for any of our ^{10}Be ages.

^{10}Be sample processing, analytical techniques, and age calculation

All samples were processed at the University at Buffalo Cosmogenic Isotope Laboratory following standard procedures from ref. 43 and a modified version of procedures used at the University of Vermont Cosmogenic Nuclide Laboratory (<http://www.uvm.edu/cosmolab/?Page=methods.html>).

$^{10}\text{Be}/^9\text{Be}$ sample ratios were measured at Center for Accelerator Mass Spectrometry, Lawrence Livermore National Laboratory (44). Bedrock and moraine boulder samples from Ayr

Lake valley, published here for the first time, were measured relative to 07KNSTD3110 with a reported $^{10}\text{Be}/^9\text{Be}$ ratio of 2.85×10^{-12} (45). Samples from the Clyde Foreland were originally reported in ref. 11 and samples from the Clyde Inlet ice-contact delta were originally reported in refs. 15 and 46; both data sets were measured relative to KNSTD3110 with a reported $^{10}\text{Be}/^9\text{Be}$ ratio of 3.15×10^{-12} (45; Table S1). We include all ^{10}Be sample information, whether previously published or not, in Table S1. One-sigma analytical uncertainties for newly presented ^{10}Be ages from Ayr Lake valley range from 1.65-3.73% (Table S1) and we use the larger of the internal vs. external AMS error when reporting uncertainties. Procedural blank ratios were 2.15×10^{-15} , 1.33×10^{-15} and 1.49×10^{-15} , corresponding to $\sim 23,330$, $14,400$ and $16,140$ atoms of ^{10}Be (<1% of sample total).

^{10}Be ages were calculated using the CRONUS-Earth online exposure age calculator (47; version 2.2, constants 2.2; Table S1). We report ^{10}Be ages using the northeastern North America (NENA) production rate (St - 3.91 ± 0.19 atoms $\text{g}^{-1} \text{yr}^{-1}$) and the commonly used constant-production scaling scheme of Lal/Stone (St; 46, 48, 49). Calculated ages using alternative scaling schemes (De, Du, Li, Lm) are shown in Table S2; all scaling schemes produce ages that agree within $\sim 2\%$ (50-53).

Using the NENA ^{10}Be production rate

The calibration data set used to generate the NENA ^{10}Be production rate includes ^{10}Be measurements from boulders on the Clyde Inlet ice-contact delta (46). Thus, there is some degree of circular logic in using the NENA rate to show that the Clyde inlet ice-contact delta, which was included in the derivation of the NENA rate, represents an ice-margin response to the 8.2 ka

event. Here, however, we present three main arguments that support our use of the NENA rate for the Clyde Inlet ^{10}Be ages:

- 1) The NENA calibration data set incorporates ^{10}Be measurements from five additional locations to generate the NENA ^{10}Be production rate. Excluding our Clyde Inlet data set from the broader suite of NENA calibration sites does not significantly alter the final NENA rate because the calculated ^{10}Be production rate based solely on the Clyde Inlet dataset ($St - 3.92 \pm 0.31 \text{ atoms g}^{-1} \text{ yr}^{-1}$) is almost identical to the NENA ^{10}Be production rate ($St - 3.91 \pm 0.19 \text{ atoms g}^{-1} \text{ yr}^{-1}$).
- 2) The NENA rate has been reproduced in nearby western Greenland, which does not include the Clyde Inlet dataset, and is statistically indistinguishable from the NENA rate (54; $St - 3.98 \pm 0.24 \text{ atoms g}^{-1} \text{ yr}^{-1}$).
- 3) Deposition of the Clyde Inlet ice-contact delta is independently constrained by bracketing radiocarbon ages of 8435 ± 50 and $7950 \pm 45 \text{ cal yr BP}$ (see below). These bracketing radiocarbon ages support the 8.2 ka age of the ice-contact delta, even when even our NENA-derived boulder ^{10}Be ages from the delta surface are not used.

Ayr Lake valley and Clyde Foreland ^{10}Be ages and chronology

Six of the eight ages from the Clyde Foreland were originally reported in ref. 11. The original publication reports over 100 exposure ages from the broader Clyde Inlet region; however, these ages come from distinct morphostratigraphic surfaces, and depending on the

sample locality have varying degrees of isotopic inheritance. Exposure ages from regions that show clear signs of scouring (e.g. valley bottoms) are generally interpreted to reflect the timing of deglaciation, whereas ages from unscoured terrain are more directly related to ice-sheet basal thermal regimes. Here, we report the ^{10}Be ages from the inner portion of the foreland, which most closely constrain the onset of deglaciation through Ayr Lake valley (see Table 1, “Upper Kogalu River valley” in ref. 11). We recalculate these previously published ^{10}Be ages using the NENA ^{10}Be production rate. We note that the Clyde Foreland samples were processed and measured by AMS between 2002-2004. These samples have analytical uncertainties that are much larger ($\sim 2x$) than newly presented ages from Ayr Lake bedrock and moraine boulders (Table S1). The significantly reduced analytical uncertainties likely reflect a combination of improved laboratory ^{10}Be extraction techniques and AMS measurement capabilities.

Nonetheless, all ^{10}Be ages from inner Clyde Foreland overlap at 1-sigma uncertainties (14.1 ± 1.2 ka) and are therefore plotted as one point in Figure 3 of the main text. In addition, the ^{10}Be ages from inner Clyde Foreland overlap with our mid-Ayr Lake valley ^{10}Be ages of 13.8 ± 0.5 , 13.6 ± 0.3 and 13.8 ± 0.2 ka (mean = 13.7 ± 0.1 ka), indicating rapid valley deglaciation, likely facilitated by increased calving rates as the glacier terminus retreated through the deep Ayr Lake (e.g. 16).

Of our 13 ^{10}Be ages from moraine boulders, 10 cluster between 8.4 ± 0.2 ka and 7.9 ± 0.2 (Fig. 3, main text). From the down-valley moraine (moraine North; Table S1), a single ^{10}Be age of 14.2 ± 0.3 ka does not overlap with remaining ^{10}Be ages at 2-sigma uncertainty. This boulder likely contains inherited ^{10}Be , and we note that this age overlaps with Ayr Lake deglaciation ages. Thus it is possible that this boulder could have originally been deposited on the landscape during Ayr Lake deglaciation, and then later transported to its present locality during the 8.2 ka-

triggered advance of the mountain glacier. At the up-valley moraine (moraine South; Table S1), a ^{10}Be age of 17.2 ± 0.3 ka does not overlap at 2-sigma uncertainty with remaining the ^{10}Be ages, indicating the presence of inherited ^{10}Be . A second older ^{10}Be age from moraine South of 9.1 ± 0.3 ka overlaps with the remaining ^{10}Be ages at 1-sigma uncertainty. However, when considering the full population of ^{10}Be ages from both moraine locations, we are confident that the 8.4-7.9 cluster (see Fig. 3, main text) accurately constrains the timing of moraine abandonment. Taken together, the ^{10}Be ages between 8.4 ± 0.2 ka and 7.9 ± 0.2 average 8.2 ± 0.2 ka (1 s.d.)

Sam Ford fiord chronology

The deglaciation chronology of Sam Ford fiord presented in Figure 3 of the main text was originally reported in ref. 16. Constraining the timing of deglaciation through Sam Ford Fiord, is a ~110 km transect of ^{10}Be and ^{14}C ages from the fiord mouth to the fiord head. The fiord mouth deglaciated at 10.3 ± 0.3 ka based on a single ^{10}Be age. With the exception of one ^{10}Be age suspected to contain inheritance (11.5 ± 0.2 ka), all ^{10}Be ages from the outer and middle portions of the fiord overlap and 1-sigma uncertainty, indicating that rapid deglaciation occurred ca. 9.5 ± 0.3 ka (n = 8, 1 s.d.). Located ~20 km from the fiord head, radiocarbon ages of 8330 ± 30 and 8210 ± 190 cal yr BP from marine bivalves in an ice-contact delta that is part of the “Ed Smith moraine,” the most prominent moraine deposited during the Cockburn Substage (13), chronicle the readvance of the Sam Ford fiord outlet glacier. Supporting a re-advance (versus a stillstand) is a radiocarbon age of $8,830 \pm 120$ cal yr BP from a bivalve reworked into a moraine up-fiord from the ice-contact delta. This older radiocarbon age requires ice-free conditions up-fiord from the ice-contact delta at that time ($8,830 \pm 120$ cal yr BP). The reworked marine

bivalve radiocarbon age serves a distant maximum-limiting age for the ice-contact delta and also indicates that following deglaciation ca. 9.5 kyr ago based on the ^{10}Be ages, the inner fiord, including ice-contact delta site, remained ice-free until the subsequent advance 8.1-8.3 kyr ago (16). ^{10}Be ages of 7.9 ± 0.8 and 7.7 ± 1.1 ~15 km up fiord from the ice-contact delta provide minimum-limiting ages on the ice-contact delta and mark the timing of final deglaciation of Sam Ford fiord (Fig. 3, main text).

Clyde Inlet ice-contact delta

^{10}Be ages from the outer portion of Clyde Inlet and radiocarbon ages from bivalves located in the middle and inner portions of the fiord indicate that Clyde Inlet deglaciated between ~11.5 and 9 ka. However, a series of ice-contact deltas and moraine ridges grading to these deltas in the inner portions of the fiord mark stable positions of the LIS outlet glacier occupying Clyde Inlet following initial deglaciation. Of particular interest are ice-contact deltas resting at 62 and 67 m asl. Moraines border their upvalley sides and distributary channels with intact boulder-levees can be found on the surfaces of the ice-contact deltas. ^{10}Be ages from boulders resting on the surface of the 62-m-asl ice-contact delta range from 7.5 ± 0.8 to 8.6 ± 0.6 ka and have a mean age of 8.0 ± 0.4 ka ($n = 7$, 1 s.d.; Table S1), which constrains the timing of delta deposition. Deposition of this delta is also independently constrained by a series of radiocarbon ages. Marine sediments are draped onto the foreslope of the 62-m-asl ice-contact delta. Because the delta must have been deposited before the marine sediments, radiocarbon ages from bivalves within the marine sediments provide minimum-limiting ages on the ice-contact delta. Three radiocarbon ages of 7790 ± 55 , 7905 ± 70 and 7950 ± 45 cal yr BP from bivalves were obtained from the foreslope sediments (Table S3; 15). These ages are in stratigraphic order and thus the oldest

(lowermost) radiocarbon age serves as the closest minimum-limiting age of the 62-m-asl ice-contact delta (7950 ± 45 cal yr BP). Maximum-limiting radiocarbon ages for the 62-m-asl ice-contact delta come from an older, higher-elevation ice-contact delta located ~ 4 km down-fiord resting at 67 m asl. A bivalve from the 67-m-asl delta was previously dated to 8735 ± 175 cal yr BP by conventional ^{14}C methods (Table S3; 55). Ref. 15, who dated a paired bivalve from the same section, obtained an AMS radiocarbon age of 8435 ± 50 cal yr BP. This AMS radiocarbon age from the 67-m-asl delta, combined with the radiocarbon ages from the marine sediments draping the foreslope of the 62-m-asl delta constrain the timing of deposition of the 62-m-asl delta to between 8435 ± 50 and 7950 ± 45 cal yr BP. This radiocarbon-based age assignment for the 62 m asl delta is indistinguishable from the age of delta deposition based on ^{10}Be ages from boulders resting on the delta surface (8.0 ± 0.4 ka).

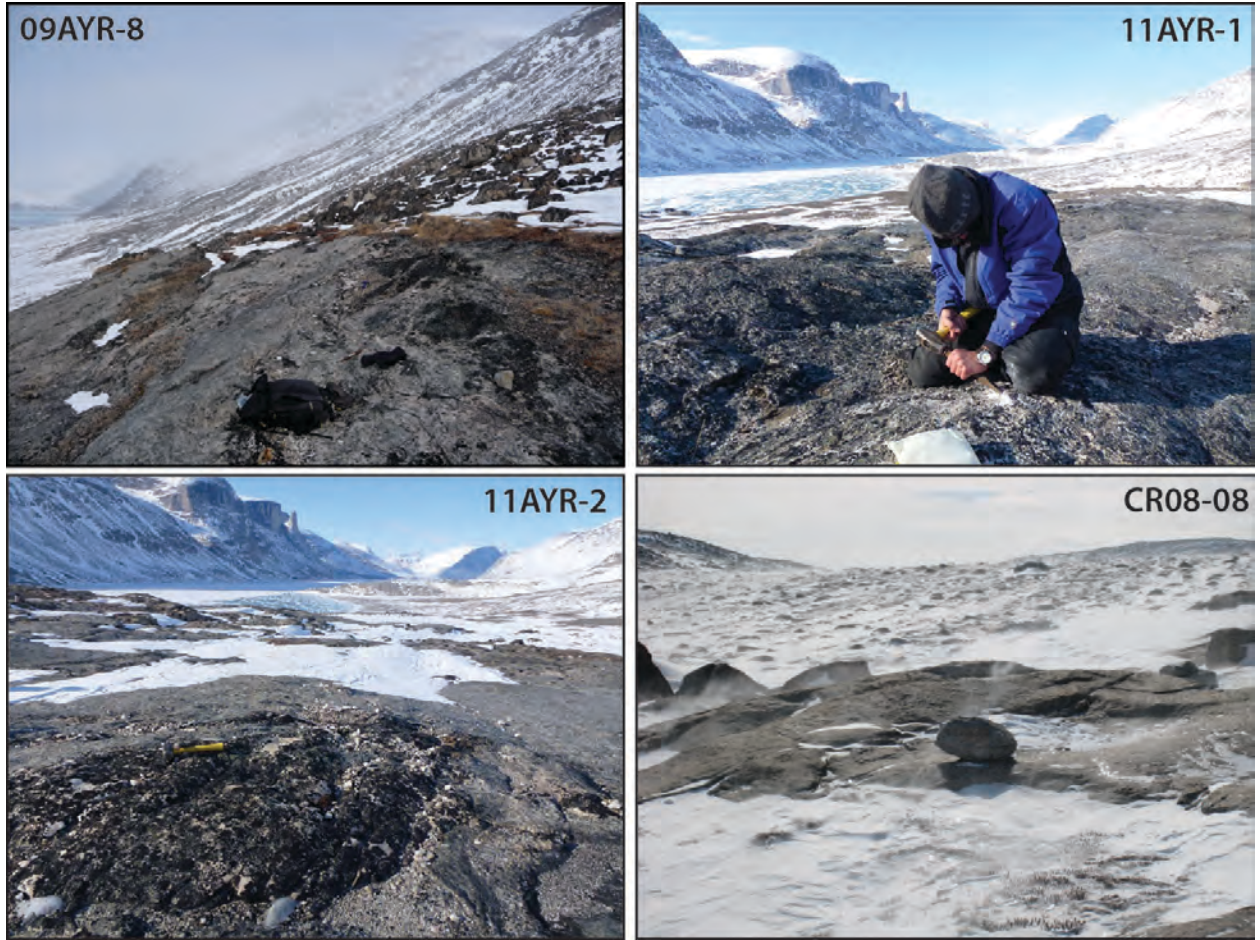


Fig. S1. Bedrock surfaces used to constrain the timing of Ayr Lake valley deglaciation.



Fig. S2. Moraine boulders from moraine North (Table S1).

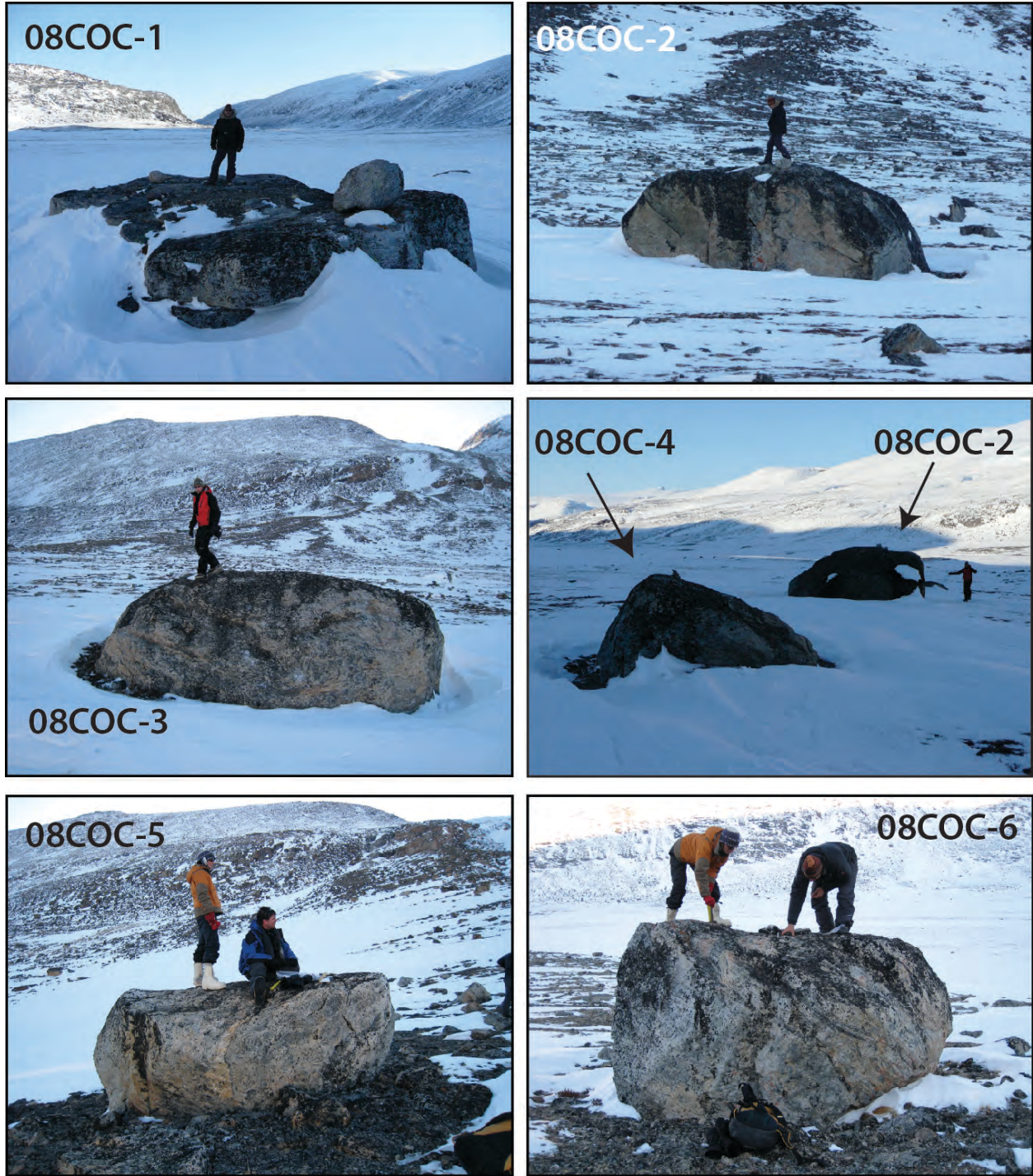


Fig. S3. Moraine boulders from moraine South (Table S1).



Fig. S4. Photograph showing the relationship between the positions of the 8.2 ka event and Little Ice Age moraines. The maximum distance between moraines in this photograph is ~300 m.

Table S1: ¹⁰Be sample information

Sample	Latitude (DD)	Longitude (DD)	Elevation (m asl)	Sample height (m)	Thickness (cm)	Shielding correction	Quartz (g)	⁹ Be carrier added (g) ^a	¹⁰ Be/ ⁹ Be ratio (10 ⁻¹³) ^b	Uncertainty (10 ⁻¹⁵)	¹⁰ Be (10 ⁴ atoms g ⁻¹)	¹⁰ Be uncertainty (10 ³ atoms g ⁻¹)	²⁶ Al (10 ⁵ atoms g ⁻¹)	²⁶ Al uncertainty (10 ⁴ atoms g ⁻¹)	¹⁰ Be age (ky) ^c	²⁶ Al age (ky)
Clyde Foreland deglaciation																
AL02-1	70.4884	-69.6583	385	0	2.0	0.594	50.45	0.38	1.30	6.38	6.52	6.16	NA	NA	15.6 ± 1.5	NA
AL02-10	70.4884	-69.6583	832	0	2.0	0.611	55.11	0.34	2.06	5.82	8.49	7.25	NA	NA	12.9 ± 1.1	NA
AL1-00-1	70.4889	-69.3539	259	cobble	7.0	0.991	41.74	0.51	0.96	3.73	7.86	7.03	4.69	4.79	13.6 ± 1.2	13.2 ± 1.4
AL4-01-1	70.5121	-68.9248	153	2.5	2.0	1.000	39.96	0.25	1.96	5.34	8.21	6.99	4.53	4.72	15.2 ± 1.3	13.6 ± 1.4
AL4-01-2	70.5068	-68.9284	172	2.0	2.0	1.000	39.14	0.25	1.64	4.65	6.99	5.98	4.76	5.30	12.6 ± 1.1	14.0 ± 1.6
CF02-107	70.6188	-69.2343	124	1.5	5.0	1.000	41.02	0.35	1.27	5.39	7.24	6.60	NA	NA	14.1 ± 1.3	NA
AL6-01-1	70.5112	-69.0381	207	2.5	2.0	1.000	40.77	0.35	2.83	6.99	16.30	13.70	NA	NA	28.4 ± 2.4	NA
AL6-01-2	70.5106	-69.0383	190	1.5	2.0	1.000	33.52	0.35	1.22	3.69	8.49	7.31	NA	NA	15.0 ± 1.3	NA
Ayr Lake valley deglaciation																
CR08-08	70.0054	-70.8933	234	bedrock	5.0	0.998	50.0425	0.4000	3.06	6.51	6.62	1.41	NA	NA	12.7 ± 0.3	NA
09AYR-8	70.2652	-70.5983	152	bedrock	4.5	0.988	60.3732	0.4001	3.64	0.13	6.54	2.36	NA	NA	13.8 ± 0.5	NA
11AYR-01	70.2392	-70.6349	127	bedrock	2.0	0.994	34.4089	0.4003	2.03	4.66	6.41	1.47	NA	NA	13.6 ± 0.3	NA
11AYR-02	70.2378	-70.63848	125	bedrock	1.0	0.994	35.0620	0.3988	2.12	3.50	6.55	1.08	NA	NA	13.8 ± 0.2	NA
Moraine - North																
09AYR-1	70.3323	-70.5832	119	3.0	3.5	0.997	60.4064	0.3999	2.17	4.10	3.89	0.74	NA	NA	8.4 ± 0.2	NA
09AYR-2	70.3324	-70.5831	135	2.5	1.0	0.997	65.0553	0.3995	2.40	4.42	4.00	0.74	NA	NA	8.3 ± 0.2	NA
09AYR-3	70.3326	-70.5833	140	1.5	2.5	0.997	65.0004	0.4000	2.34	6.86	3.89	1.14	NA	NA	8.1 ± 0.2	NA
09AYR-4	70.3260	-70.6074	134	2.75	1.5	0.997	86.2288	0.3000	4.25	8.18	4.01	0.93	NA	NA	8.4 ± 0.2	NA
09AYR-5	70.3279	-70.6124	150	1.25	1.0	0.997	86.3799	0.3004	4.27	7.28	4.03	0.93	NA	NA	8.2 ± 0.2	NA
09AYR-6	70.3292	-70.6134	150	2.75	3.0	0.996	60.5013	0.4010	3.81	8.94	6.84	1.60	NA	NA	14.2 ± 0.3	NA
09AYR-7	70.3293	-70.6133	158	2.5	4.0	0.996	51.6566	0.4001	1.84	3.80	3.86	0.80	NA	NA	8.0 ± 0.2	NA
Moraine - South																
08COC-1	70.1524	-70.7339	130	1.5	2.0	0.991	60.0094	0.4000	2.39	6.70	4.32	1.21	NA	NA	9.1 ± 0.3	NA
08COC-2	70.1533	-70.7387	142	2.5	4.0	0.995	60.0832	0.4010	2.08	6.01	3.76	1.09	NA	NA	7.9 ± 0.2	NA
08COC-3	70.1533	-70.7392	142	2.0	1.5	0.995	60.0317	0.3998	2.23	8.33	4.02	1.50	NA	NA	8.3 ± 0.3	NA
08COC-4	70.1528	-70.7401	142	1.25	2.0	0.995	60.0368	0.4003	4.57	8.79	8.25	1.59	NA	NA	17.2 ± 0.3	NA
08COC-5	70.1546	-70.7486	186	1.5	3.0	0.992	55.3751	0.4000	2.08	3.97	4.07	0.78	NA	NA	8.1 ± 0.2	NA
08COC-6	70.1529	-70.7433	166	1.75	2.5	0.995	52.1322	0.4005	1.97	4.64	4.09	0.97	NA	NA	8.2 ± 0.2	NA
Clyde Inlet: ice-contact delta																
CI2-01-1	69.8353	-70.4970	65	2.0	5.0	1.000	61.45	0.57	0.56	6.34	3.59	3.90	NA	NA	7.5 ± 0.8	NA
CI2-01-2	69.8345	-70.4980	65	2.0	4.0	1.000	52.06	0.47	0.61	6.32	3.83	3.80	NA	NA	7.9 ± 0.8	NA
CR03-90	69.8302	-70.4962	72	1.3	2.0	1.000	26.76	0.35	0.48	3.60	4.02	3.40	NA	NA	8.1 ± 0.7	NA
CR03-91	69.8318	-70.4958	67	1.1	2.0	1.000	28.3041	0.3430	0.46	3.44	3.70	3.00	NA	NA	7.5 ± 0.6	NA
CR03-92	69.8318	-70.4958	67	1.5	2.0	1.000	52.9147	0.3449	0.92	5.37	4.02	2.60	NA	NA	8.2 ± 0.5	NA
CR03-93	69.8324	-70.4967	67	1.6	3.0	1.000	41.3262	0.3467	0.73	3.56	4.11	2.30	NA	NA	8.4 ± 0.5	NA
CR03-94	69.8328	-70.4975	65	1.3	2.0	1.000	40.2615	0.3537	0.70	4.60	4.23	2.90	NA	NA	8.6 ± 0.6	NA

^a Ayr Lake valley deglaciation, moraine North and moraine South samples were spiked with a 405µg/g ⁹Be carrier. Samples from Clyde Foreland and Clyde Inlet were spiked with SPEX 1000 µg/g ⁹Be carrier. Quartz and carrier weights only reported to the 2nd decimal place were measured on a 2-digit balance.

^b AMS analyses for samples from the Clyde Foreland and Clyde Inlet are standardized to KNSTD3110 (3.15 × 10⁻¹²) and were completed in 2002-2004, all remaining samples are standardized to 07KNSTD3110 (2.85 × 10⁻¹²); ratios are blank-corrected (<1% of sample total) and shown at 1-sigma AMS uncertainty

^c ¹⁰Be ages given in ky at 1-sigma AMS uncertainties. Ages were calculated using the CRONUS Earth online calculator (v 2.2, constants 2.2), NENA production rate (3.91 ± 0.19 at/g/yr SLHL), St scaling, standard atmospheric pressure, "0" erosion, and a sample density of 2.65 g cm³.

Table S2: ¹⁰Be ages (ky) using alternative scaling schemes

Sample	St (from S1)	De	Du	Li	Lm
<i>Clyde Foreland deglaciation</i>					
AL02-1	15.6 ± 1.5	15.6 ± 1.5	15.4 ± 1.5	15.2 ± 1.5	15.9 ± 1.5
AL02-10	12.9 ± 1.1	12.9 ± 1.1	12.7 ± 1.1	12.5 ± 1.1	13.1 ± 1.1
AL1-00-1	13.6 ± 1.2	13.5 ± 1.2	13.3 ± 1.2	13.2 ± 1.2	13.8 ± 1.2
AL4-01-1	15.2 ± 1.3	15.0 ± 1.3	14.7 ± 1.3	14.6 ± 1.3	15.4 ± 1.3
AL4-01-2	12.6 ± 1.1	12.5 ± 1.1	12.3 ± 1.1	12.2 ± 1.1	12.8 ± 1.1
CF02-107	14.1 ± 1.3	13.9 ± 1.3	13.7 ± 1.3	13.6 ± 1.3	14.3 ± 1.3
AL6-01-1	28.4 ± 2.4	28.1 ± 2.4	27.7 ± 2.4	27.3 ± 2.4	28.8 ± 2.4
AL6-01-2	15.0 ± 1.3	14.9 ± 1.3	14.6 ± 1.3	14.5 ± 1.3	15.3 ± 1.3
<i>Ayr Lake valley deglaciation</i>					
CR08-08	12.7 ± 0.3	12.6 ± 0.3	12.4 ± 0.3	12.4 ± 0.3	12.9 ± 0.3
09AYR-8	13.8 ± 0.5	13.6 ± 0.5	13.4 ± 0.5	13.3 ± 0.5	14.0 ± 0.5
11AYR-01	13.6 ± 0.3	13.3 ± 0.3	13.1 ± 0.3	13.1 ± 0.3	13.8 ± 0.3
11AYR-02	13.8 ± 0.2	13.5 ± 0.2	13.3 ± 0.2	13.3 ± 0.2	14.0 ± 0.2
<i>Moraine - North</i>					
09AYR-1	8.4 ± 0.2	8.2 ± 0.2	8.1 ± 0.2	8.0 ± 0.2	8.5 ± 0.2
09AYR-2	8.3 ± 0.2	8.1 ± 0.2	8.0 ± 0.2	8.0 ± 0.2	8.4 ± 0.2
09AYR-3	8.1 ± 0.2	8.0 ± 0.2	7.9 ± 0.2	7.8 ± 0.2	8.2 ± 0.2
09AYR-4	8.4 ± 0.2	8.2 ± 0.2	8.1 ± 0.2	8.0 ± 0.2	8.5 ± 0.2
09AYR-5	8.2 ± 0.2	8.1 ± 0.2	8.0 ± 0.2	7.9 ± 0.2	8.3 ± 0.2
09AYR-6	14.2 ± 0.3	14.0 ± 0.3	13.8 ± 0.3	13.7 ± 0.3	14.4 ± 0.3
09AYR-7	8.0 ± 0.2	7.9 ± 0.2	7.8 ± 0.2	7.7 ± 0.2	8.1 ± 0.2
<i>Moraine - South</i>					
08COC-1	9.1 ± 0.3	9.0 ± 0.3	8.8 ± 0.3	8.8 ± 0.3	9.3 ± 0.3
08COC-2	7.9 ± 0.2	7.8 ± 0.2	7.7 ± 0.2	7.6 ± 0.2	8.1 ± 0.2
08COC-3	8.3 ± 0.3	8.2 ± 0.3	8.1 ± 0.3	8.0 ± 0.3	8.4 ± 0.3
08COC-4	17.2 ± 0.3	16.9 ± 0.3	16.7 ± 0.3	16.5 ± 0.3	17.4 ± 0.3
08COC-5	8.1 ± 0.2	8.0 ± 0.2	7.9 ± 0.2	7.9 ± 0.2	8.3 ± 0.2
08COC-6	8.2 ± 0.2	8.1 ± 0.2	8.0 ± 0.2	7.9 ± 0.2	8.4 ± 0.2
<i>Clyde Inlet: ice-contact delta</i>					
CI2-01-1	7.5 ± 0.8	7.3 ± 0.8	7.2 ± 0.8	7.2 ± 0.8	7.6 ± 0.8
CI2-01-2	7.9 ± 0.8	7.7 ± 0.8	7.6 ± 0.8	7.6 ± 0.8	8.0 ± 0.8
CR03-90	8.1 ± 0.7	7.9 ± 0.7	7.8 ± 0.7	7.8 ± 0.7	8.2 ± 0.7
CR03-91	7.5 ± 0.6	7.3 ± 0.6	7.2 ± 0.6	7.2 ± 0.6	7.6 ± 0.6
CR03-92	8.2 ± 0.5	8.0 ± 0.5	7.9 ± 0.5	7.8 ± 0.5	8.3 ± 0.5
CR03-93	8.4 ± 0.5	8.2 ± 0.5	8.1 ± 0.5	8.0 ± 0.5	8.5 ± 0.5
CR03-94	8.6 ± 0.6	8.4 ± 0.6	8.3 ± 0.6	8.2 ± 0.6	8.7 ± 0.6

¹⁰Be ages (ky) at 1-sigma interal AMS uncertainties using St, De, Du, Li, and Lm scaling schemes.

Table S3: Radiocarbon ages

Sample	Sample type and context	Latitude (N)	Longitude (W)	¹⁴ C age (¹⁴ C yr BP ± 1 SD) ^a	Calibrated age (cal yr. BP ± 1 SD) ^b	Reference
Clyde Inlet						
I-1932	bivalve in ice-contact delta	69.87°	70.47°	8340 ± 130 ^a	8735 ± 175	Andrews and Draiper, 1967
CURL-7044	bivalve in ice-contact delta	69.87°	70.43°	8120 ± 40	8435 ± 50	Briner et al., 2007
CURL-7039	bivalve	69.83°	70.50°	7470 ± 40	7790 ± 55	Briner et al., 2007
AA-45381	bivalve	69.83°	70.50°	7590 ± 70	7905 ± 70	Briner et al., 2007
CURL-7038	bivalve	69.83°	70.50°	7620 ± 40	7950 ± 45	Briner et al., 2007
Sam Ford Fiord						
I-1553	bivalve in ice-contact delta	70.21°	71.29°	7910 ± 200 ^a	8210 ± 205	Andrews and Draiper, 1967
SF07-SH01	bivalve in ice-contact delta	70.21°	71.29°	8000 ± 20	8340 ± 25	Briner et al., 2009

^a410 yr was added because ¹⁴C ages were originally reported with an assumed δ ¹³C of -25 per mil instead of 0 per mil.

^bRadiocarbon ages were calibrated using CALIB 6.0. A locally calibrated 540 yr (delta R = 140 yr) reservoir correction was applied to all bivalves following Briner et al. (2007).

References

1. R. B. Alley *et al.*, Holocene climatic instability: A prominent, widespread event 8200 yr ago. *Geology* **25**, 483 (1997). [doi:10.1130/0091-7613\(1997\)025<0483:HCIAPW>2.3.CO;2](https://doi.org/10.1130/0091-7613(1997)025<0483:HCIAPW>2.3.CO;2)
2. J. Severinghaus, T. Sowers, E. J. Brook, R. B. P. Alley, M. L. Bender, *Nature* **391**, 141 (1998). [doi:10.1038/34346](https://doi.org/10.1038/34346)
3. R. B. Alley, A. M. Ágústadóttir, The 8k event: Cause and consequences of a major Holocene abrupt climate change. *Quat. Sci. Rev.* **24**, 1123 (2005). [doi:10.1016/j.quascirev.2004.12.004](https://doi.org/10.1016/j.quascirev.2004.12.004)
4. M. R. Kaplan *et al.*, Glacier retreat in New Zealand during the Younger Dryas stadial. *Nature* **467**, 194 (2010). [doi:10.1038/nature09313](https://doi.org/10.1038/nature09313)
5. S. Björck *et al.*, Anomalously mild Younger Dryas summer conditions in southern Greenland. *Geology* **30**, 427 (2002). [doi:10.1130/0091-7613\(2002\)030<0427:AMYDSC>2.0.CO;2](https://doi.org/10.1130/0091-7613(2002)030<0427:AMYDSC>2.0.CO;2)
6. G. H. Denton, R. B. Alley, G. C. Comer, W. S. Broecker, The role of seasonality in abrupt climate change. *Quat. Sci. Rev.* **24**, 1159 (2005). [doi:10.1016/j.quascirev.2004.12.002](https://doi.org/10.1016/j.quascirev.2004.12.002)
7. M. A. Kelly *et al.*, A ¹⁰Be chronology of lateglacial and Holocene mountain glaciation in the Scoresby Sund region, east Greenland: Implications for seasonality during lateglacial time. *Quat. Sci. Rev.* **27**, 2273 (2008). [doi:10.1016/j.quascirev.2008.08.004](https://doi.org/10.1016/j.quascirev.2008.08.004)
8. O. S. Lohne, J. Mangerud, J. I. Svendsen, Timing of the younger dryas glacial maximum in western Norway. *J. Quat. Sci.* **27**, 81 (2012). [doi:10.1002/jqs.1516](https://doi.org/10.1002/jqs.1516)
9. G. Falconer, J. T. Andrews, J. D. Ives, Late-Wisconsin End Moraines in Northern Canada. *Science* **147**, 608 (1965). [doi:10.1126/science.147.3658.608](https://doi.org/10.1126/science.147.3658.608) [Medline](#)
10. G. H. Miller, A. S. Dyke, Proposed Extent of Late Wisconsin Laurentide Ice on Eastern Baffin Island. *Geology* **2**, 125 (1974). [doi:10.1130/0091-7613\(1974\)2<125:PEOLWL>2.0.CO;2](https://doi.org/10.1130/0091-7613(1974)2<125:PEOLWL>2.0.CO;2)
11. J. P. Briner, G. H. Miller, P. T. Davis, R. C. Finkel, Cosmogenic exposure dating in arctic glacial landscapes: implications for the glacial history of northeastern Baffin Island, Arctic Canada. *Can. J. Earth Sci.* **42**, 67 (2005). [doi:10.1139/e04-102](https://doi.org/10.1139/e04-102)
12. J. P. Briner, G. H. Miller, P. Thompson Davis, R. C. Finkel, Cosmogenic radionuclides from fiord landscapes support differential erosion by overriding ice sheets. *Geol. Soc. Am. Bull.* **118**, 406 (2006). [doi:10.1130/B25716.1](https://doi.org/10.1130/B25716.1)
13. J. T. Andrews, J. D. Ives, “Cockburn” Nomenclature and the Late Quaternary History of the Eastern Canadian Arctic. *Arct. Alp. Res.* **10**, 617 (1978). [doi:10.2307/1550683](https://doi.org/10.2307/1550683)
14. Materials and methods are available as supplementary materials on *Science* Online
15. J. P. Briner, I. Overeem, G. Miller, R. Finkel, The deglaciation of Clyde Inlet, northeastern Baffin Island, Arctic Canada. *J. Quat Sci* **22**, 223 (2007). [doi:10.1002/jqs.1057](https://doi.org/10.1002/jqs.1057)
16. J. P. Briner, A. C. Bini, R. S. Anderson, Rapid early Holocene retreat of a Laurentide outlet glacier through an Arctic fjord. *Nat. Geosci.* **2**, 496 (2009). [doi:10.1038/ngeo556](https://doi.org/10.1038/ngeo556)
17. J. E. Smith, Sam Ford Fiord: A study in deglaciation. Thesis, McGill University, Montreal (1966).

18. N. E. Young *et al.*, Response of a marine-terminating Greenland outlet glacier to abrupt cooling 8200 and 9300 years ago. *Geophys. Res. Lett.* **38**, L24701 (2011).
[doi:10.1029/2011GL049639](https://doi.org/10.1029/2011GL049639)
19. A. E. Putnam *et al.*, Glacier advance in southern middle-latitudes during the Antarctic Cold Reversal. *Nat. Geosci.* **3**, 700 (2010). [doi:10.1038/ngeo962](https://doi.org/10.1038/ngeo962)
20. Y. Axford, J. P. Briner, G. H. Miller, D. Francis, Paleoecological evidence for abrupt cold reversals during peak Holocene warmth on Baffin Island, Arctic Canada. *Quat. Res.* **71**, 142 (2009). [doi:10.1016/j.yqres.2008.09.006](https://doi.org/10.1016/j.yqres.2008.09.006)
21. R. M. Koerner, Mass balance of glaciers in the Queen Elizabeth Islands, Nunavut, Canada. *Ann. Glaciol.* **42**, 417 (2005). [doi:10.3189/172756405781813122](https://doi.org/10.3189/172756405781813122)
22. W. R. Kapsner, R. B. Alley, C. A. Shuman, S. Anandkrishnan, P. M. Grootes, Dominant influence of atmospheric circulation on snow accumulation in Greenland over the past 18,000 years. *Nature* **373**, 52 (1995). [doi:10.1038/373052a0](https://doi.org/10.1038/373052a0)
23. R. B. Alley, The Younger Dryas cold interval as viewed from central Greenland. *Quat. Sci. Rev.* **19**, 213 (2000). [doi:10.1016/S0277-3791\(99\)00062-1](https://doi.org/10.1016/S0277-3791(99)00062-1)
24. J. Oerlemans, *Glaciers and Climate Change* (A. A. Balkema Publishers, Lisse, 2001).
25. R. B. Alley, Comment on “When Earth’s freezer door is left ajar”. *Eos Trans.* **84**, 315 (2003). [doi:10.1029/2003EO330004](https://doi.org/10.1029/2003EO330004)
26. T. Kobashi, J. P. Severinghaus, E. J. Brook, J. M. Barnola, A. M. Grachev, Precise timing and characterization of abrupt climate change 8200 years ago from air trapped in polar ice. *Quat. Sci. Rev.* **26**, 1212 (2007). [doi:10.1016/j.quascirev.2007.01.009](https://doi.org/10.1016/j.quascirev.2007.01.009)
27. B. M. Vinther *et al.*, Holocene thinning of the Greenland ice sheet. *Nature* **461**, 385 (2009).
[doi:10.1038/nature08355](https://doi.org/10.1038/nature08355) [Medline](#)
28. W. S. Broecker *et al.*, Putting the Younger Dryas cold event into context. *Quat. Sci. Rev.* **29**, 1078 (2010). [doi:10.1016/j.quascirev.2010.02.019](https://doi.org/10.1016/j.quascirev.2010.02.019)
29. D. C. Barber *et al.*, *Nature* **400**, 344 (1999). [doi:10.1038/22504](https://doi.org/10.1038/22504)
30. T. V. Lowell *et al.*, Testing the Lake Agassiz meltwater trigger for the Younger Dryas. *Eos Trans* **86**, 365 (2005). [doi:10.1029/2005EO400001](https://doi.org/10.1029/2005EO400001)
31. J. T. Andrews *et al.*, A Heinrich-like event, H-0 (DC-0): Source(s) for detrital carbonate in the North Atlantic during the Younger Dryas Chronozone. *Paleoceanpgraphy* **10**, 943 (1995). [doi:10.1029/95PA01426](https://doi.org/10.1029/95PA01426)
32. H. Cheng *et al.*, Ice age terminations. *Science* **326**, 248 (2009). [doi:10.1126/science.1177840](https://doi.org/10.1126/science.1177840)
[Medline](#)
33. A. Born, A. Levermann, The 8.2 ka event: Abrupt transition of the subpolar gyre toward a modern North Atlantic circulation. *Geochem. Geophys. Geosyst.* **11**, Q06011 (2010).
[doi:10.1029/2009GC003024](https://doi.org/10.1029/2009GC003024)
34. C. Hillaire-Marcel, A. de Vernal, D. J. W. Piper, Lake Agassiz Final drainage event in the northwest North Atlantic. *Geophys. Res. Lett.* **34**, L15601 (2007).
[doi:10.1029/2007GL030396](https://doi.org/10.1029/2007GL030396)

35. A. S. Dyke *et al.*, The Laurentide and Innuitian ice sheets during the Last Glacial Maximum. *Quat. Sci. Rev.* **21**, 9 (2002). [doi:10.1016/S0277-3791\(01\)00095-6](https://doi.org/10.1016/S0277-3791(01)00095-6)
36. S. O. Rasmussen *et al.*, A new Greenland ice core chronology for the last glacial termination. *J. Geophys. Res.* **111**, (D6), D06102 (2006). [doi:10.1029/2005JD006079](https://doi.org/10.1029/2005JD006079)
37. G. D. Jackson *et al.*, Geology, Clyde River, District of Franklin: Geological Survey of Canada, "A" Series Map 1582A, scale 1:250,000 (1984).
38. D. E. Sugden, *J. Glaciol.* **20**, 367 (1978).
39. J. P. Briner, G. H. Miller, P. T. Davis, P. R. Bierman, M. Caffee, Last Glacial Maximum ice sheet dynamics in Arctic Canada inferred from young erratics perched on ancient tors. *Quat. Sci. Rev.* **22**, 437 (2003). [doi:10.1016/S0277-3791\(03\)00003-9](https://doi.org/10.1016/S0277-3791(03)00003-9)
40. J. P. Briner, G. H. Miller, R. Finkel, D. P. Hess, Glacial erosion at the fjord onset zone and implications for the organization of ice flow on Baffin Island, Arctic Canada. *Geomorphology* **97**, 126 (2008). [doi:10.1016/j.geomorph.2007.02.039](https://doi.org/10.1016/j.geomorph.2007.02.039)
41. P. T. Davis, J. P. Briner, R. D. Coulthard, R. W. Finkel, G. H. Miller, Preservation of Arctic landscapes overridden by cold-based ice sheets. *Quat. Res.* **65**, 156 (2006). [doi:10.1016/j.yqres.2005.08.019](https://doi.org/10.1016/j.yqres.2005.08.019)
42. B. M. Goehring *et al.*, Late glacial and holocene ^{10}Be production rates for western Norway. *J. Quat Sci* **27**, 89 (2012). [doi:10.1002/jqs.1517](https://doi.org/10.1002/jqs.1517)
43. C. P. Kohl, K. Nishiizumi, Chemical isolation of quartz for measurement of in-situ -produced cosmogenic nuclides. *Geochim. Cosmochim. Acta* **56**, 3583 (1992). [doi:10.1016/0016-7037\(92\)90401-4](https://doi.org/10.1016/0016-7037(92)90401-4)
44. D. H. Rood, S. Hall, T. P. Guilderson, R. C. Finkel, T. A. Brown, Challenges and opportunities in high-precision Be-10 measurements at CAMS. *Nucl. Instrum. Meth. B* **268**, 730 (2010). [doi:10.1016/j.nimb.2009.10.016](https://doi.org/10.1016/j.nimb.2009.10.016)
45. K. Nishiizumi *et al.*, Absolute calibration of ^{10}Be AMS standards. *Nucl. Instrum. Meth. B.* **258**, 403 (2007). [doi:10.1016/j.nimb.2007.01.297](https://doi.org/10.1016/j.nimb.2007.01.297)
46. G. Balco *et al.*, Regional beryllium-10 production rate calibration for late-glacial northeastern North America. *Quat. Geochronol.* **4**, 93 (2009). [doi:10.1016/j.quageo.2008.09.001](https://doi.org/10.1016/j.quageo.2008.09.001)
47. G. Balco, J. O. Stone, N. A. Lifton, T. J. Dunai, A complete and easily accessible means of calculating surface exposure ages or erosion rates from ^{10}Be and ^{26}Al measurements. *Quat. Geochronol.* **3**, 174 (2008). [doi:10.1016/j.quageo.2007.12.001](https://doi.org/10.1016/j.quageo.2007.12.001)
48. D. Lal, Cosmic ray labeling of erosion surfaces: in situ nuclide production rates and erosion models. *Earth Planet. Sci. Lett.* **104**, 424 (1991). [doi:10.1016/0012-821X\(91\)90220-C](https://doi.org/10.1016/0012-821X(91)90220-C)
49. J. O. Stone, Air pressure and cosmogenic isotope production. *J. Geophys. Res.* **105**, (B10), 23753 (2000). [doi:10.1029/2000JB900181](https://doi.org/10.1029/2000JB900181)
50. N. A. Lifton *et al.*, Addressing solar modulation and long-term uncertainties in scaling secondary cosmic rays for in situ cosmogenic nuclide applications. *Earth Planet. Sci. Lett.* **239**, 140 (2005). [doi:10.1016/j.epsl.2005.07.001](https://doi.org/10.1016/j.epsl.2005.07.001)

51. D. Desilets, M. Zreda, Spatial and temporal distribution of secondary cosmic-ray nucleon intensities and applications to in situ cosmogenic dating. *Earth Planet. Sci. Lett.* **206**, 21 (2003). [doi:10.1016/S0012-821X\(02\)01088-9](https://doi.org/10.1016/S0012-821X(02)01088-9)
52. D. Desilets, M. Zreda, T. Prabu, Extended scaling factors for in situ cosmogenic nuclides: New measurements at low latitude. *Earth Planet. Sci. Lett.* **246**, 265 (2006). [doi:10.1016/j.epsl.2006.03.051](https://doi.org/10.1016/j.epsl.2006.03.051)
53. T. J. Dunai, Influence of secular variation of the geomagnetic field on production rates of in situ produced cosmogenic nuclides. *Earth Planet. Sci. Lett.* **193**, 197 (2001). [doi:10.1016/S0012-821X\(01\)00503-9](https://doi.org/10.1016/S0012-821X(01)00503-9)
54. J. P. Briner, N. E. Young, B. M. Goehring, J. M. Schaefer, Constraining Holocene ^{10}Be production rates in Greenland. *J. Quat Sci.* **27**, 2 (2012). [doi:10.1002/jqs.1562](https://doi.org/10.1002/jqs.1562)
55. J. T. Andrews, L. Draiper, *Geogr. Bull.* **9**, 115 (1967).